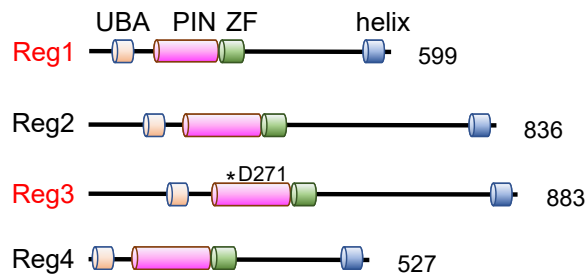
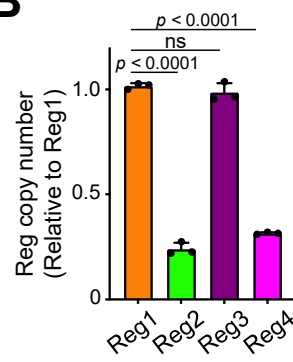
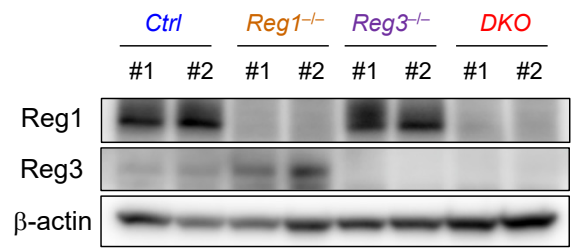
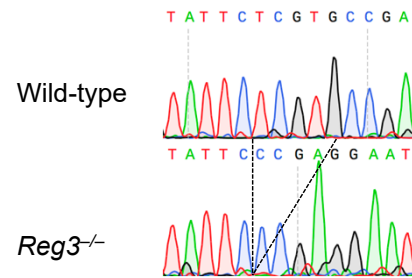
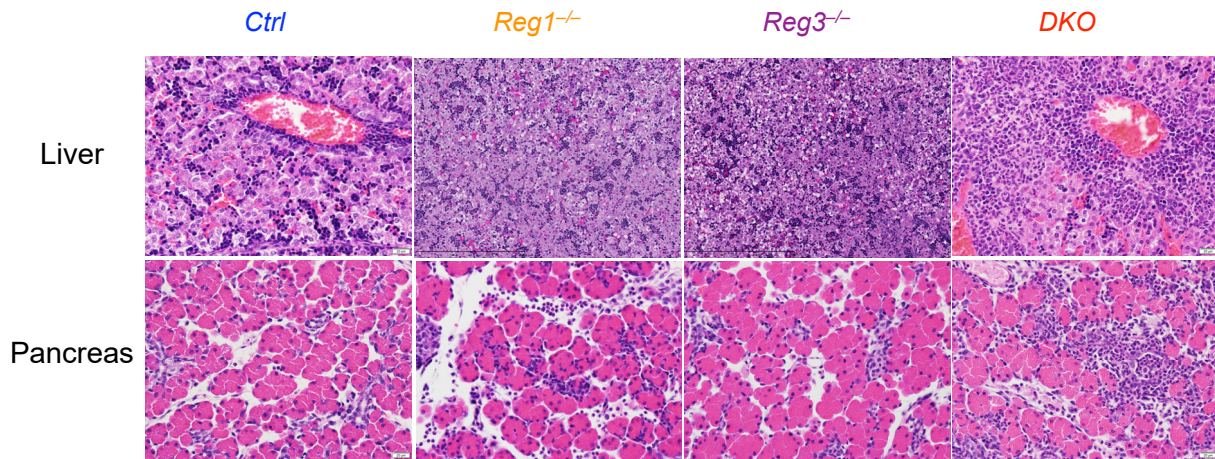
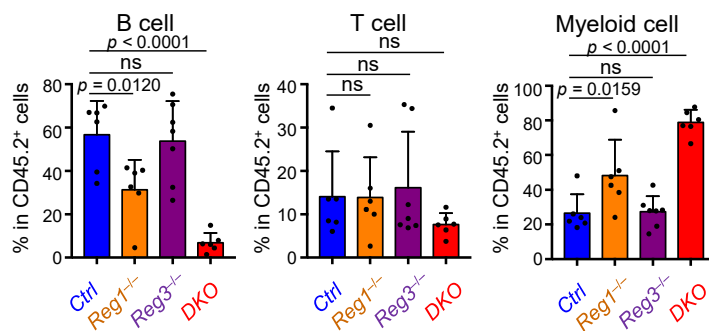
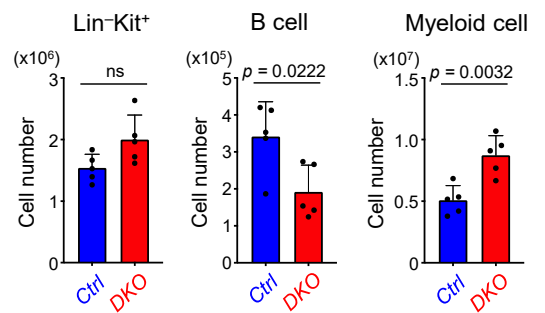
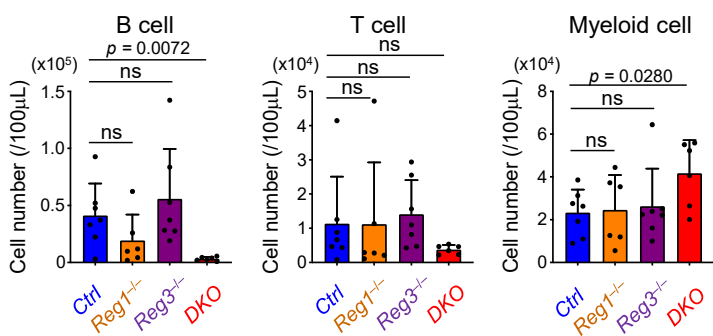
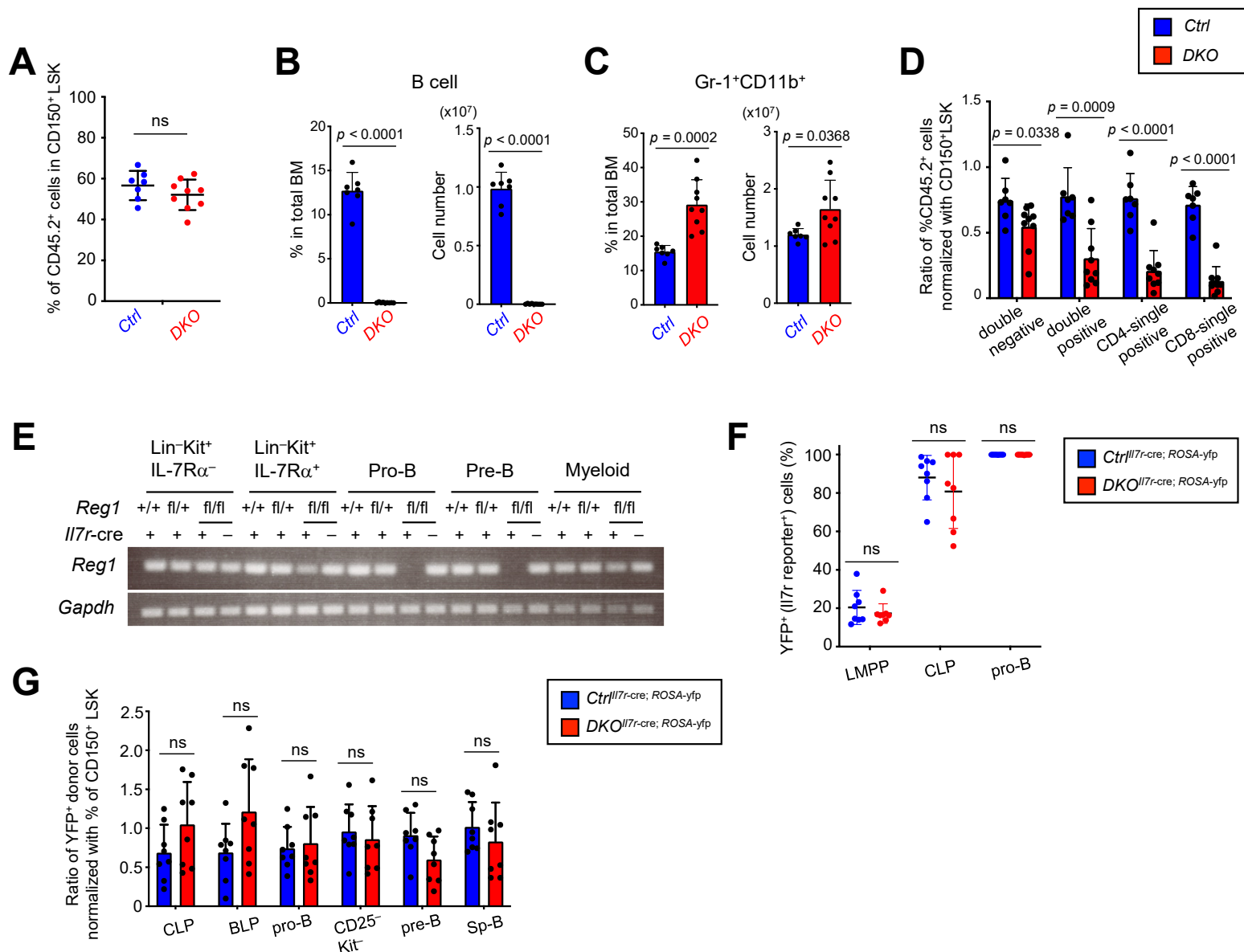
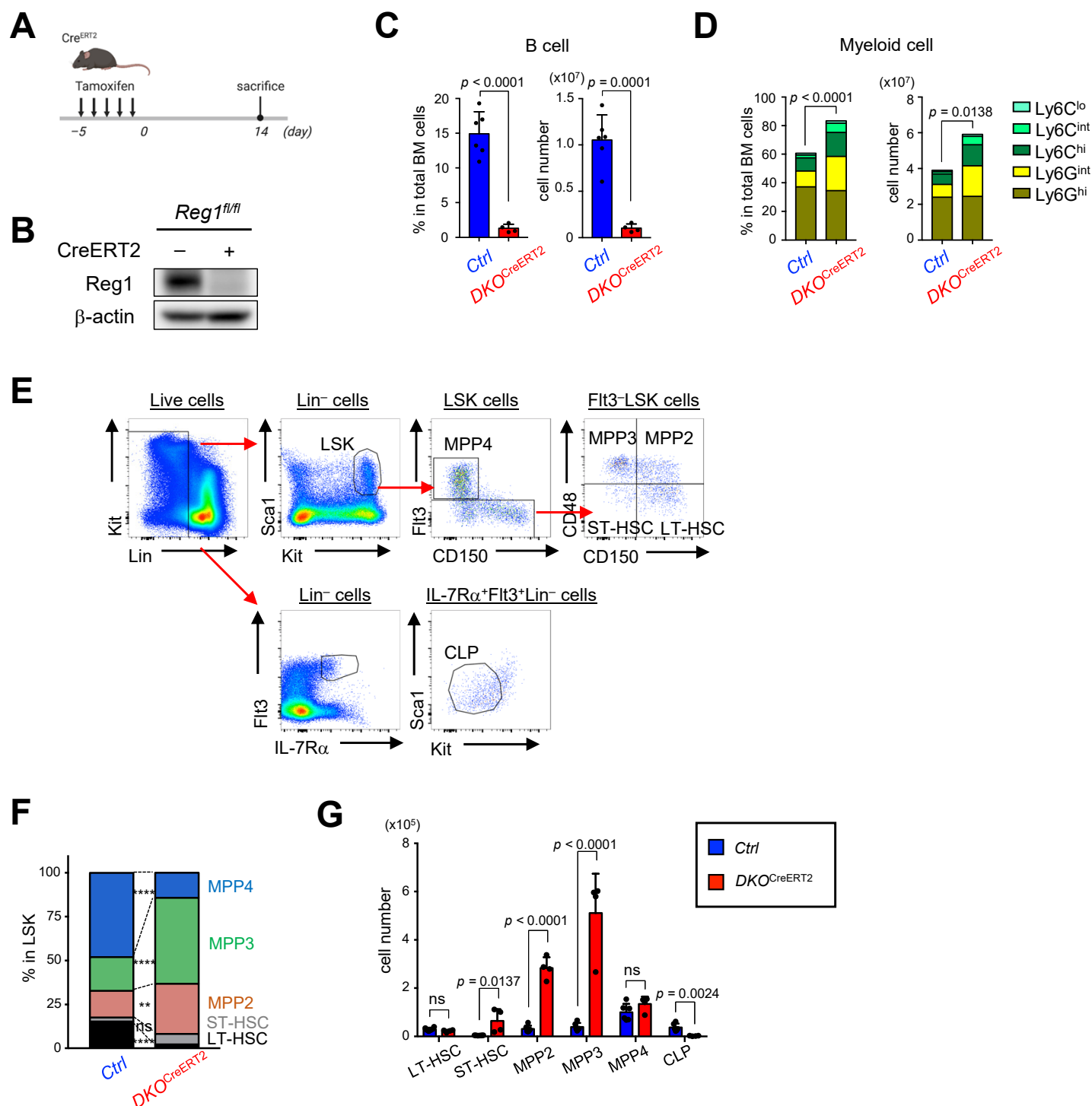


**A****B****C****D****E****F****G****I****H**

**Supplemental Figure 1. Double deficiency of *Reg1* and *Reg3* causes neonatal lethality accompanied by the neutrophil infiltration in the liver and pancreas** (A) Schematic representation of domain structures for Reg family proteins. Asterisk in Reg3 represents the position of amino acid essential for nuclease activity. (B) Relative expression levels of Regnase family genes in bone marrow (BM) lineage-negative (Lin<sup>-</sup>) cells (n = 3). Copy numbers of Regnase family genes were normalized to Reg1 copy number. (C) Immunoblot analysis of Reg1 and Reg3 in Lin<sup>-</sup> cells from mice reconstituted with fetal liver (FL) cells of the indicated genotypes. (D) Schematic representation of strategy for generation of *Reg3*<sup>-/-</sup> mice by CRISPR-Cas9 system. (E) 5-mer deletion within exon 3 of *Reg3* locus in the mutant allele. (F) H&E staining of liver and pancreas from neonates. (G-H) Percentages and cell numbers of donor B cells (CD19<sup>+</sup>B220<sup>+</sup>), T cells (CD4/8<sup>+</sup>TCRβ<sup>+</sup>), and myeloid cells (CD19<sup>-</sup>CD11b<sup>+</sup>) in the peripheral blood from FL-transplanted mice (*Ctrl*, n = 6; *Reg1*<sup>-/-</sup>, n = 6; *Reg3*<sup>-/-</sup>, n = 7; *DKO*, n = 6). Mice (CD45.1) reconstituted with FL cells of the indicated genotypes (CD45.2) were analyzed 4-6 weeks post-transplantation, shown in Figure 1A. (I) Cell numbers of Lin<sup>-</sup>Kit<sup>+</sup> progenitors, CD19<sup>+</sup>B220<sup>+</sup> cells, and CD19<sup>-</sup>B220<sup>-</sup>Myeloid markers<sup>+</sup> (CD11b/CD11c/Gr-1/DX5) cells in the FL of E15.5 fetuses of the indicated genotypes. (*Ctrl*, n = 5; *DKO*, n = 5). Data are representative of two independent experiments (B, C, G-I). Bar graphs are presented as mean ± SD (G-I). Statistical significance was calculated by one-way ANOVA with Holm-Sidak multiple comparisons test (G, H). Unpaired two-tailed Student's *t*-test (I). ns, not significant.



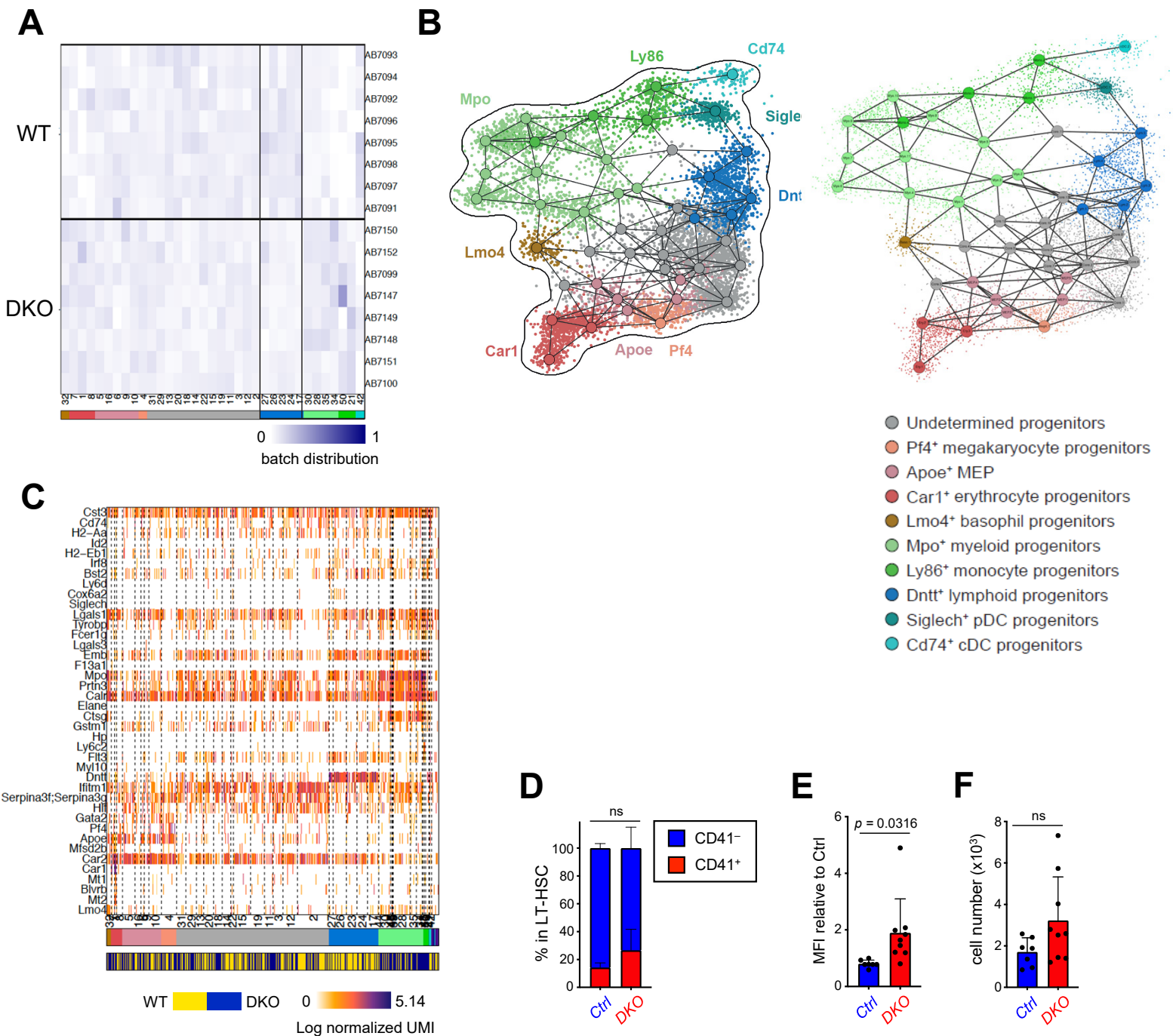
**Supplemental Figure 2. Deletion of *Reg1* and *Reg3* resulted in a profound defect in T/B lymphopoiesis in a cell-intrinsic manner (A-D)** Competitive transplantation of control (*Ctrl*) or *Reg1*<sup>-/-</sup>*Reg3*<sup>-/-</sup> (*DKO*) FL cells (CD45.2) together with competitors (CD45.1) (*Ctrl*,  $n = 7$ ; *DKO*,  $n = 9$ ). (A) Percentages of CD45.2<sup>+</sup> cells in SLAMF6<sup>+</sup>LSK population from FL-reconstituted mice. (B-C) Frequencies and cell numbers of CD19<sup>+</sup> B220<sup>+</sup> and Gr-1<sup>+</sup> CD11b<sup>+</sup> cells in the BM of FL competitively-transplanted mice (D) Thymic development of FL-transplanted mice. Each dot represents the ratio of the percentage of CD45.2 in each population to the percentage of CD45.2 in CD150<sup>+</sup> LSK from a single recipient mouse. (E) RT-PCR analysis of *Reg1* in FL cells from fetuses of the indicated genotypes. RNA was prepared from Lin-Kit<sup>+</sup>IL-7R $\alpha$ <sup>-</sup>, Lin-Kit<sup>+</sup>IL-7R $\alpha$ <sup>+</sup>, Pro-B, Pre-B, and CD11b<sup>+</sup> myeloid lineage cells. (F) Percentages of YFP<sup>+</sup> cells in donor cells (CD45.2) from mice competitively transplanted with FL cells from *Il7r-cre*<sup>+</sup>ROSA<sup>yfp/+</sup>*Reg1*<sup>fl/+</sup>*Reg3*<sup>+/-</sup> (*Ctrl*<sup>Il7r-cre</sup>) or *Il7r-cre*<sup>+</sup>ROSA<sup>yfp/+</sup>*Reg1*<sup>fl/fl</sup>*Reg3*<sup>-/-</sup> (*DKO*<sup>Il7r-cre</sup>) fetuses (CD45.2) along with *Il7r-cre*<sup>+</sup>ROSA<sup>yfp/+</sup> fetuses (CD45.1/45.2) ( $n = 8$ , each). (G) B cell development of mice competitively transplanted as in (F). Each dot represents the ratio of the percentage of CD45.2 in YFP<sup>+</sup> donor cells of each population to the percentage of CD45.2 in CD150<sup>+</sup> LSK from a single recipient mouse. Data are a composite of three independent experiments. Data are representative of two (E) of three (A-D, F) independent experiments. Data are presented as mean  $\pm$  SD (A-D, F-G). Statistical significance was calculated by unpaired two-tailed Student's *t*-test.



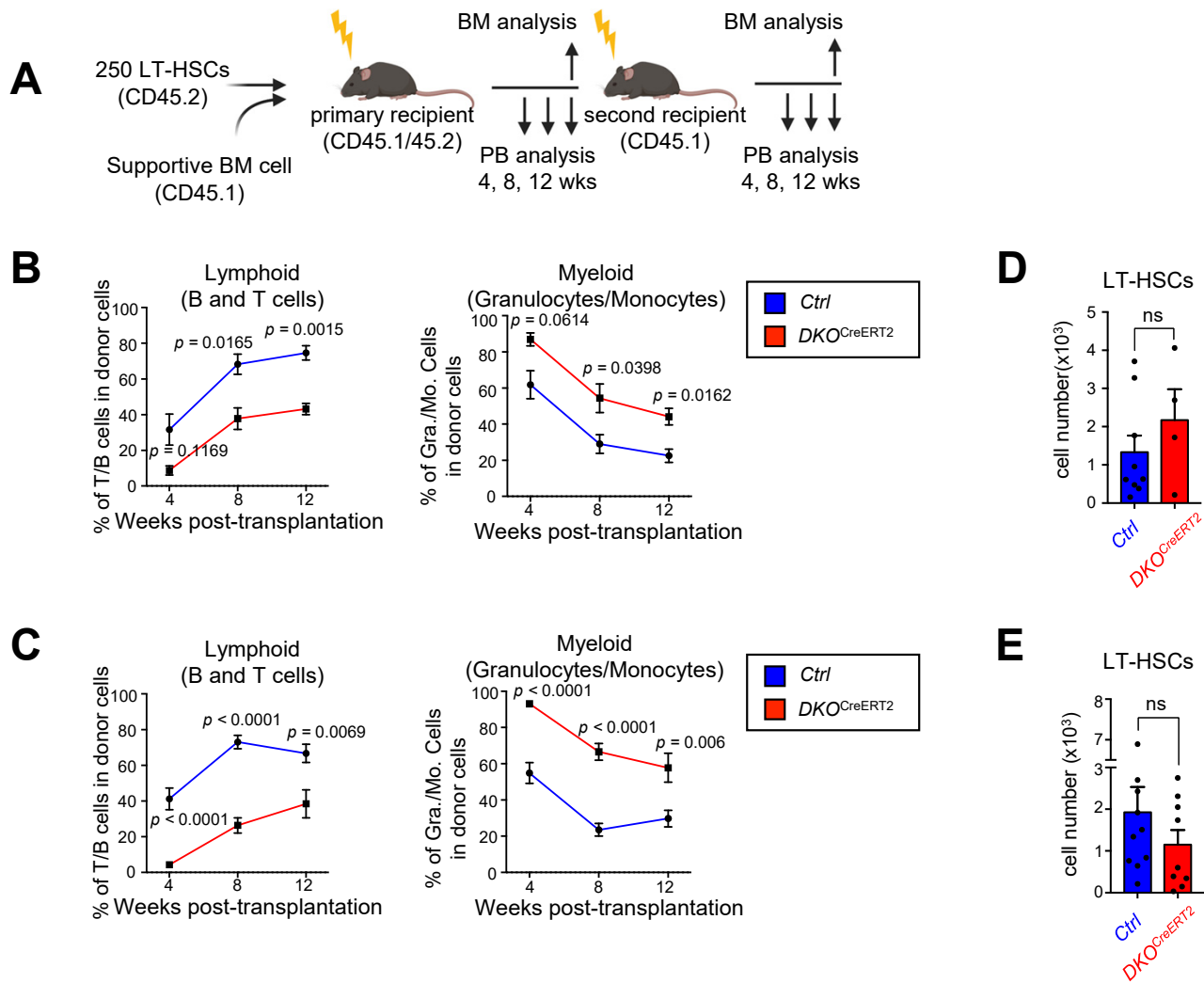
### Supplemental Figure 3. Inducible deletion of *Reg1* in the absence of *Reg3* results in altered hematopoiesis favoring myeloid lineages

(A) Experimental design for *in vivo* tamoxifen injection. (B) Immunoblot analysis of *Reg1* in Lin<sup>-</sup> BM cells from CreERT2<sup>-</sup> and CreERT2<sup>+</sup>*Reg1*<sup>fl/fl</sup> mice. BM cells were harvested from mice at day 3 after tamoxifen treatment. (C-D) frequencies and cell numbers of B220<sup>+</sup>CD19<sup>+</sup> B cells and CD11b<sup>+</sup> myeloid cells in the BM of *Ctrl* and CreERT2<sup>+</sup>*Reg1*<sup>fl/fl</sup>*Reg3*<sup>-/-</sup> (*DKO*<sup>CreERT2</sup>) mice. *n* = 6, *Ctrl*; *n* = 4, *DKO*<sup>CreERT2</sup>. (E) Gating strategy of HSPCs. LT-HSC, Flt3-CD48-CD150<sup>+</sup> LSK; ST-HSC, Flt3-CD48-CD150<sup>-</sup> LSK; MPP2, Flt3-CD48<sup>+</sup>CD150<sup>+</sup> LSK; MPP3, Flt3-CD48<sup>+</sup>CD150<sup>-</sup> LSK; MPP4, Flt3<sup>+</sup>CD48<sup>+</sup>CD150<sup>-</sup> LSK; CLP, Lin<sup>-</sup>Flt3<sup>+</sup>IL-7Rα<sup>+</sup>Sca1<sup>dull</sup>Kit<sup>dull</sup>. (F) Cell type distribution of HSPCs in *Ctrl* and *DKO*<sup>CreERT2</sup> mice. (G) Cell numbers of HSPC subpopulations in *Ctrl* and *DKO*<sup>CreERT2</sup> mice. Error bars denote the mean ± SD. \**p* < 0.05; \*\**p* < 0.01; \*\*\**p* < 0.001; \*\*\*\**p* < 0.0001. Unpaired two-tailed Student's *t*-test. ns, not significant.





**Supplemental Figure 4. Deletion of *Reg1* and *Reg3* skews gene expression patterns toward myeloid and Meg-E lineage signatures in HSPCs** (A) Enrichment of meta-cell clusters across the 384 plates of WT and DKO cells (eight plates in each genotype). Lower bar indicates meta-cell clusters. (B) A two-dimensional representation of the reference model of the hematopoietic core constructed from 8,395 BM myeloid progenitors grouped into meta-cells (left panel), as reported previously (Giladi et al. 2018). Metacell analysis enables the identification of “meta-cells,” which represent smaller subgroups within a cluster sharing similar transcriptional profiles. This methodology helps distinguish between closely related cell types or states that might otherwise be merged into a single cluster when using conventional clustering techniques (Also see supplemental methods). The number of each metacell was depicted in the core map (right panel, also see Supplemental Table S3). Cells are colored by expression of functional markers. (C) Single-cell gene expression profiles. Color bar: upper, annotation of meta-cells (see Methods) and lower, genetic backgrounds (yellow; WT, blue; DKO). (D-F) frequency and MFI of CD41 in LT-HSCs (CD45.2) and cell number of CD41<sup>+</sup> LT-HSCs (CD45.2) from competitively transplanted mice. *Ctrl*,  $n = 7$ ; *DKO*,  $n = 9$ . Error bars denote the mean  $\pm$  SD (D-F). Unpaired two-tailed Student’s *t*-test. ns, not significant.



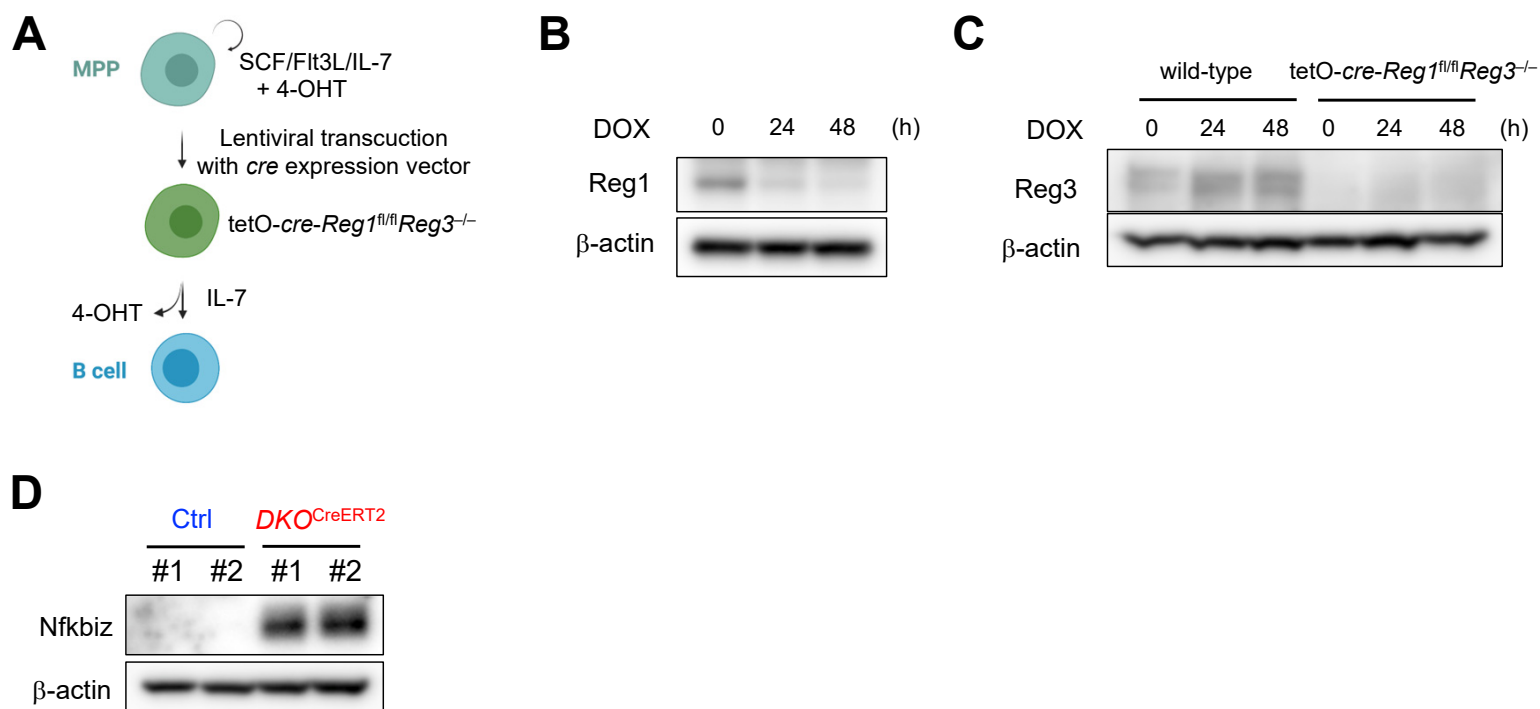
### Supplemental Figure 5. *Reg1/Reg3*-deficient HSCs exhibit myeloid-biased output upon serial transplantation

(A) Experimental schematic for primary and secondary transplantations. Recipient mice (CD45.1/CD45.2) were lethally irradiated and competitively transplanted with 250 LT-HSCs from *Ctrl* and *CreERT2<sup>+</sup>Reg1<sup>fl/fl</sup>Reg3<sup>-/-</sup>* ( $DKO^{CreERT2}$ ) mice (CD45.2) treated with tamoxifen. For secondary transplants, 1 million whole BM cells were transferred from primary recipient mice to secondary recipient mice (CD45.1). (B-C) Reconstitution potential and hematopoietic outputs after primary and second transplantation. Donor-derived lymphoid and myeloid outcomes in the peripheral blood. (D-E) Cell numbers of donor-derived LT-HSCs following primary and secondary transplantation. ((D) *Ctrl*,  $n = 9$ ;  $DKO^{CreERT2}$ ,  $n = 4$ ) ((E) *Ctrl*,  $n = 10$ ;  $DKO^{CreERT2}$ ,  $n = 9$ ) Error bars denote the mean  $\pm$  SD (D, E) or  $\pm$  SEM (B, C). Unpaired two-tailed Student's *t*-test. ns, not significant.

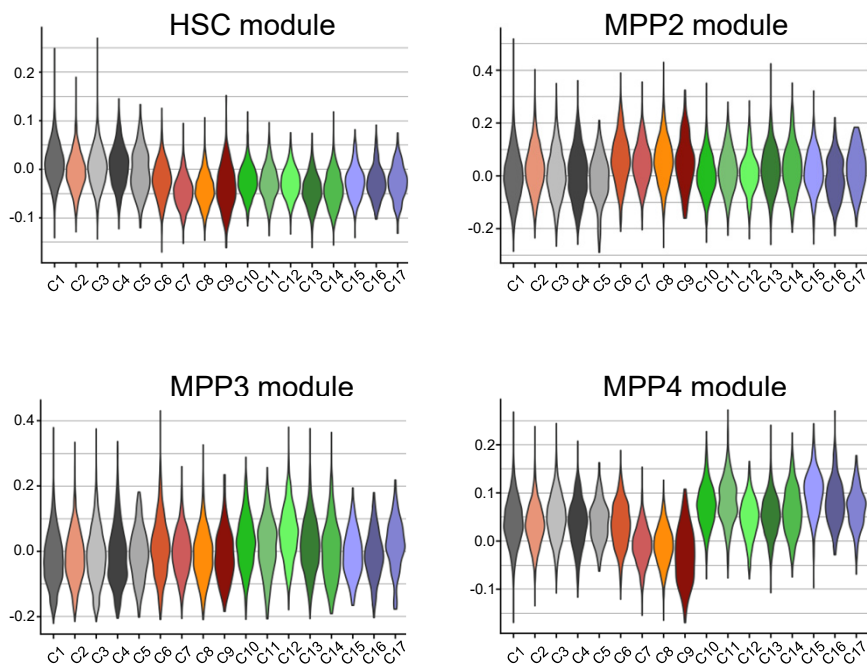
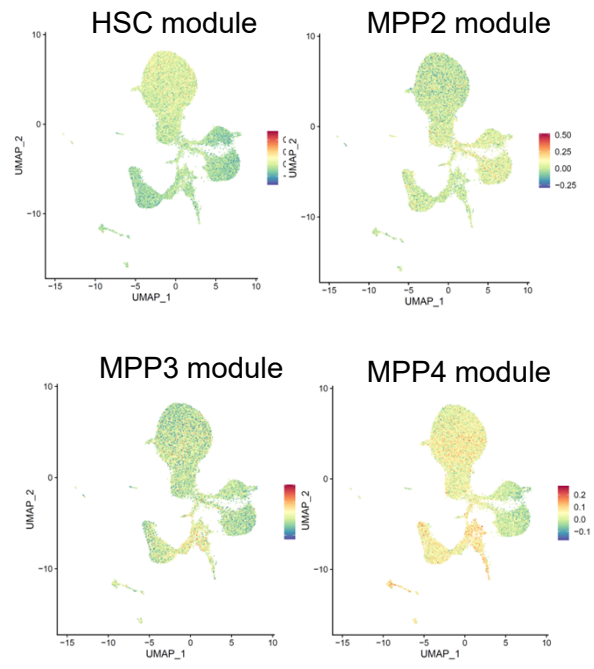
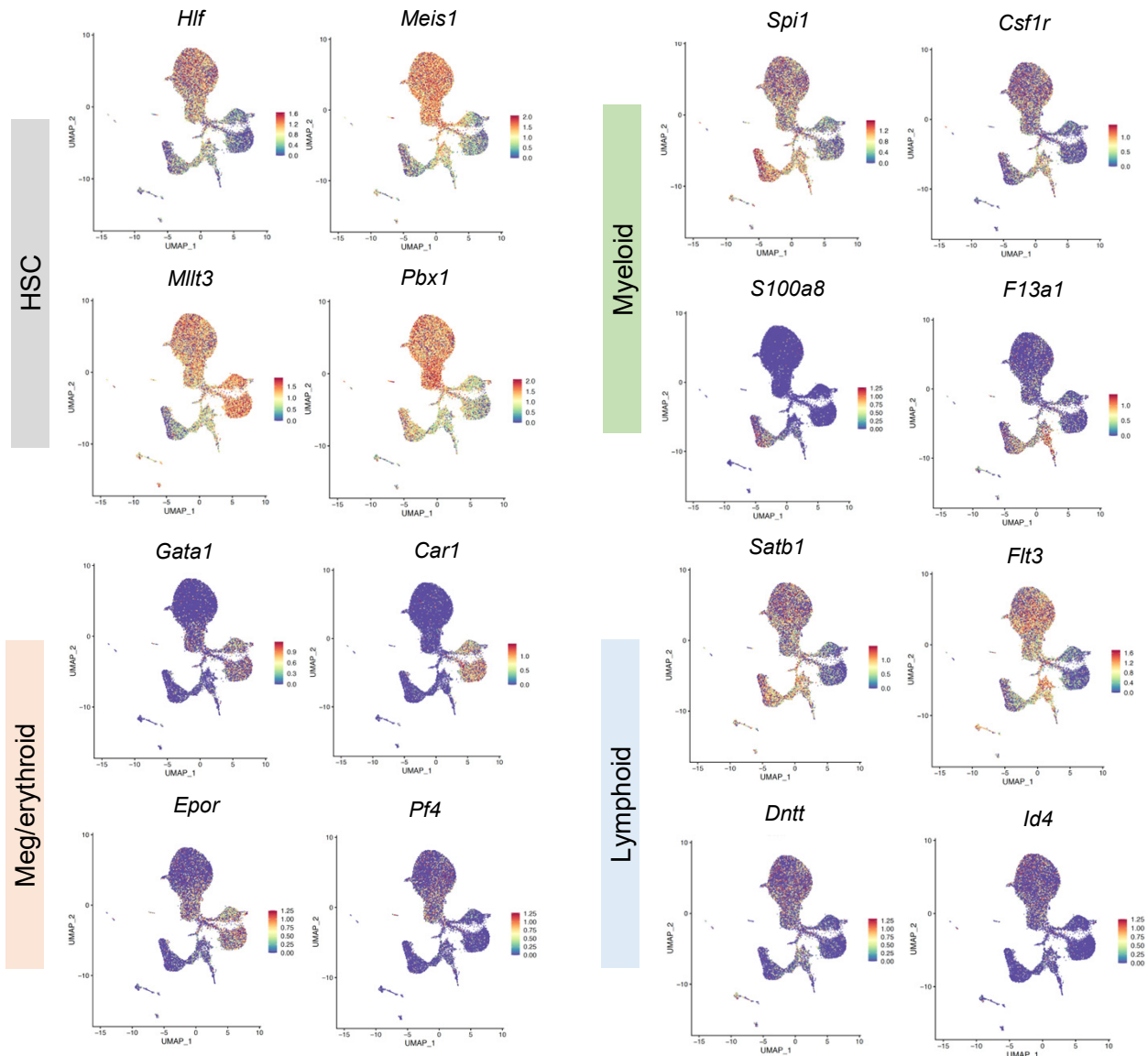


**Supplemental Figure 6. Nfkbiz is upregulated in HSPCs lacking *Reg1* and *Reg3*** (A) Heatmap showing the 9 selected genes differentially expressed in DKO cells in the scRNA-seq data (supplemental Figure 4). (B) Expression levels of the indicated genes in CD150<sup>+</sup> LSK cells and LMPP derived from mice competitively transplanted with wild-type (*Ctrl*, CD45.1) and *Reg1*<sup>-/-</sup> *Reg3*<sup>-/-</sup> (*DKO*, CD45.2) FL cells. *Ctrl* and *DKO* cells were sorted separately based on congenic markers (n = 4 each). Transcript levels were determined by quantitative RT-PCR. Data are a composite of two independent experiments. (C) Luciferase activity was assessed by using pGL3 plasmids containing 3'UTR of *Irf8* and *Cebpd*, together with mock or plasmids for wild-type or nuclease-dead mutant for *Reg1* and *Reg3* (n = 3 each). (D) mRNA stability of *Irf8* and *Cebpd* in Lin<sup>-</sup> cells from control and *DKO*<sup>CreERT2</sup> mice. Cells were stimulated with IL-1 $\beta$  for 2 hours, followed by addition of actinomycin D (ActD). The remaining transcripts relative to the 0 h time point were measured by quantitative RT-PCR. Data are representative of two independent experiments (C, D) or a composite of two experiments (A). Data are presented as mean  $\pm$  SD (A, C) or SEM (D). Statistical significance was calculated by unpaired two-tailed Student's *t*-test. ns, not significant.

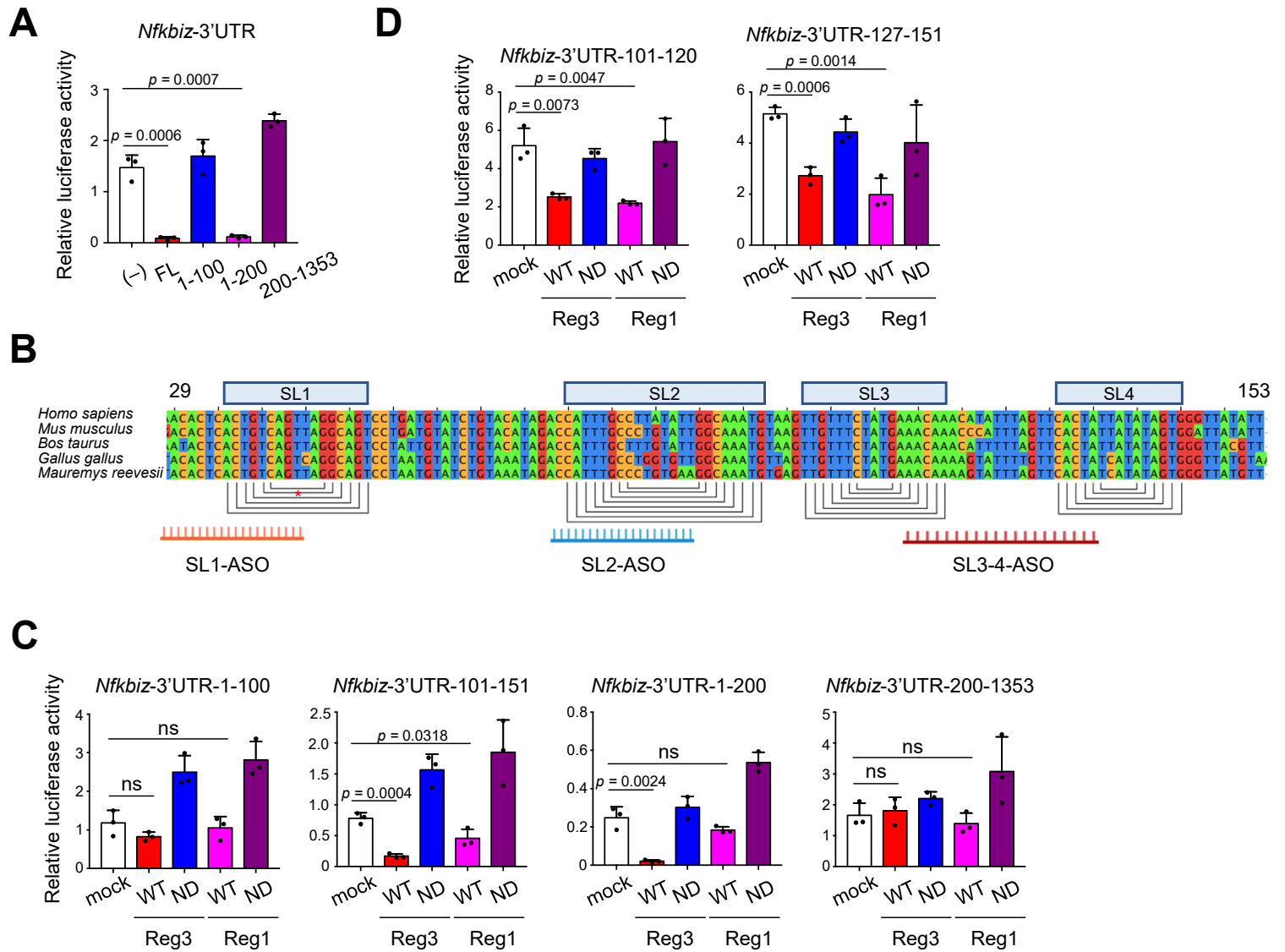




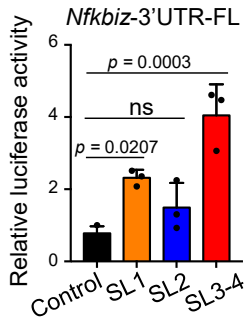
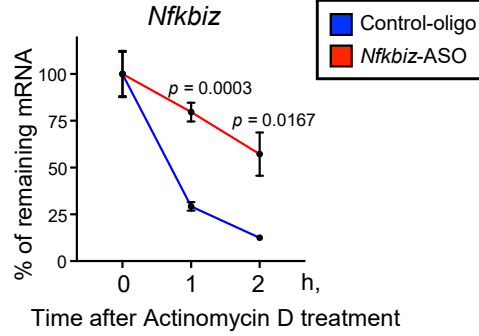
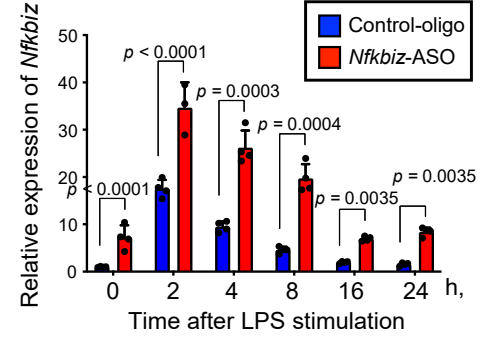
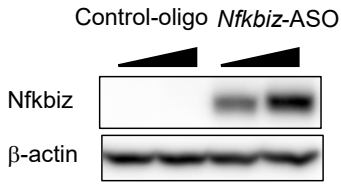
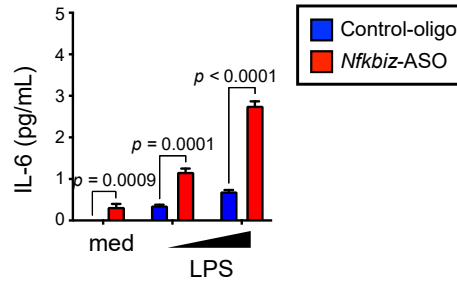
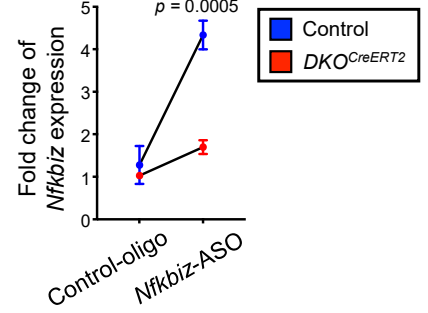
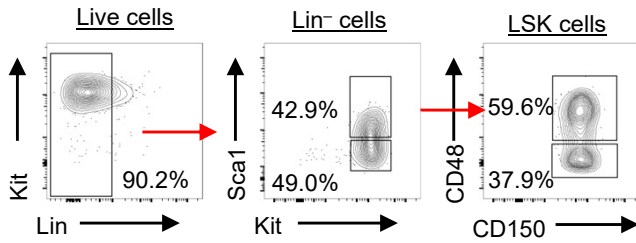
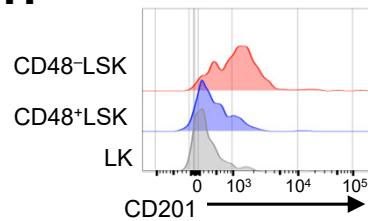
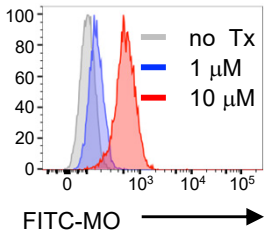
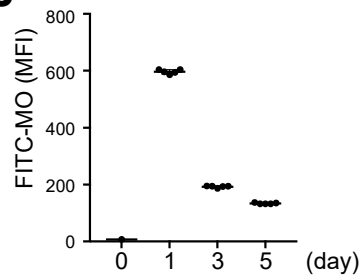
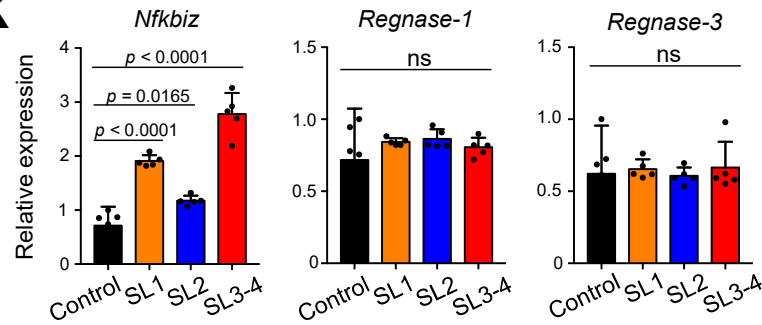
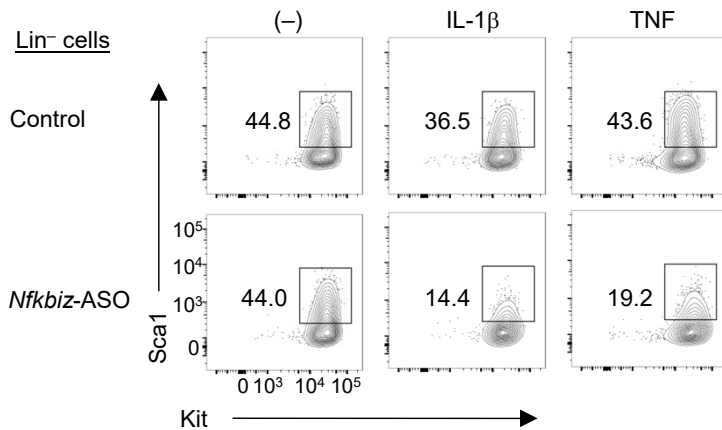
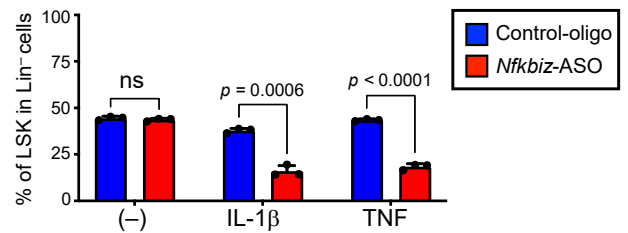
**Supplemental Figure 7. Nfkbiz is upregulated in HSPCs lacking *Reg1* and *Reg3*** (A) (D) Schematic representation for establishment of tetO-cre-Reg1<sup>fl/fl</sup>Reg3<sup>-/-</sup> MPP<sup>hId3-ERT2</sup> cells. (E-F) Immunoblot analysis of Reg1 and Reg3 in tetO-cre-Reg1<sup>fl/fl</sup>Reg3<sup>-/-</sup> MPP<sup>hId3-ERT2</sup> cells following addition of DOX. (G) Immunoblot analysis of Nfkbiz in Lin<sup>-</sup> cells from control and CreERT2<sup>+</sup>Reg1<sup>fl/fl</sup>Reg3<sup>-/-</sup> (DKO<sup>CreERT2</sup>) mice at day 3 after tamoxifen injection. Data are representative of two independent experiments (B, C, E-G) or a composite of two experiments (A). Data are presented as mean  $\pm$  SD (A-B) or SEM (C). Statistical significance was calculated by unpaired two-tailed Student's *t*-test. ns, not significant.

**A****B****C**

**Supplemental Figure 8. Single-cell ATAC-seq generated clusters characterized by distinct patterns of chromatin accessibility in Flt3-CD48-LSK cells** (A) Violin plots showing the chromatin accessibility of signature gene sets for HSC, MPP2, MPP3, and MPP4 across all scATAC-seq clusters. (B) UMAP plots showing the chromatin accessibility of signature gene sets for HSC, MPP2, MPP3, and MPP4. (C) UMAP plots showing normalized chromatin accessibility of the selected signature genes for stemness and lineage specification.



**Supplemental Figure 9. *Nfkbiz*-3'UTR 101-151 region is essential for destabilization by Reg1 and Reg3** (A) Luciferase activity of HeLa cells transfected with pGL3 plasmids containing various lengths of 3'UTR of mouse *Nfkbiz* (n = 3 each). (B) Schematic representation of Reg1/Reg3-recognition sequences and potential SL structures (SL1-4) in mouse *Nfkbiz* together with an alignment of four other species. SL structures were predicted by RNAfold. Single strand oligonucleotides against the indicated SL structures are shown at the bottom. Asterisk indicates a mismatch base pair. (C) Luciferase activity of HeLa cells transfected with pGL3 plasmids containing a set of *Nfkbiz* 3'UTR as in a,, together with expression plasmids for wild-type (WT) or nuclease-dead (ND) mutant of Reg1 and Reg3 (n = 3 each). (D) Luciferase activity of HeLa cells transfected with pGL3-βGlo plasmids containing the 101-120 or 127-151 of *Nfkbiz* 3'UTR together with expression plasmids for WT or ND mutant of Reg1 and Reg3 (n = 3 each). Bar graphs are presented as mean  $\pm$  SD (A, C, D). Unpaired two-tailed Student's *t*-test. ns, not significant. Data are representative from three independent experiments (A, C, D).

**A****B****C****D****E****F****G****H****I****J****K****L****M**

**Supplemental Figure 10. Manipulation of *Nfkbiz* expression modulates lineage bias in HSCs** (A) Luciferase activity of HeLa cells transfected with pGL3 plasmid containing full length of mouse *Nfkbiz* 3'UTR, along with a set of ASOs targeting its stem loop structures (n = 3 in SL1, SL2, and SL3-4). (B) The mRNA stability of *Nfkbiz* transcript was measured by qRT-PCR. 24 hours after transfection with Control oligo or *Nfkbiz*-targeting ASO, bone marrow-derived macrophages (BMDMs) were stimulated with LPS (100 ng/mL) for 2 hours, followed by treatment with actinomycin D (5 µg/mL) for the indicated time points (n = 4 each). (C) qRT-PCR analysis of *Nfkbiz* in BMDMs transfected with Control oligo or *Nfkbiz*-targeting ASO, then stimulated with LPS (100 ng/mL) at the indicated time points (n = 3 each). (D) Immunoblot analysis of *Nfkbiz* in BMDMs 24 hours after transfection with Control oligo or *Nfkbiz*-targeting ASO. (E) IL-6 production of BMDMs stimulated with LPS (10 or 100 ng/mL). Cells were transfected with ASOs (n = 3 each). (F) Fold change of *Nfkbiz* expression in DKO BMDMs comparing WT cells, transfected with ASOs (n = 3 each). (G) Flow cytometry plots of cultured HSCs. Please refer to Method. (H) Histogram of CD201 expression in CD48<sup>-</sup> and CD48<sup>+</sup> LSK populations from cultured HSCs. (I, J) Representative histogram of FITC-conjugated morpholino oligonucleotide (MO) in cultured HSCs at 24 hours after electroporation (I). MFI of FITC-MO in cultured HSCs was monitored by flow cytometry at the indicated time points (J) (n = 3 each). (K) quantitative RT-PCR analysis for *Nfkbiz*, *Reg1*, and *Reg3* in cultured HSCs treated with control oligo or SL-targeting ASOs (n = 5 each). (L, M) Representative flow cytometry plots and frequency of LSK population in cultured HSCs 24 hours after electroporation with control oligo or *Nfkbiz*-targeting ASO. Cells were then stimulated with IL-1β (25 ng/mL) or TNF (1 µg/mL) for 24 hours (n = 3 each). Data are presented as mean ± SD (A, C, E, F, K, M) or SEM (B). Statistical significance was calculated by one-way ANOVA with Holm-Sidak multiple comparisons test (A, K) or unpaired two-tailed Student's *t*-test (B, C, E, F, M). ns, not significant. Data are a representative from two independent experiments.



## SUPPLEMENTAL INFORMATION

### Supplementary Method details

#### Animals

*Regnase-3*-deficient (*Reg3*<sup>-/-</sup>) mice were generated by CRISPR-Cas9 technology. Guide RNA targeting exon 3 of the *Reg3* locus was injected into zygotes (gRNA sequence: AAAGAAGTATTCTCGTGCCG). *Nfkbiz* flox mice<sup>1</sup> and *Il7rCre R26R-EYFP* mice<sup>2</sup> were kindly provided by T. Maruyama and HR. Rodewald, respectively. *Regnase-1*<sup>-/-3</sup> and *Regnase-1* flox<sup>4</sup> mice were bred in our own animal colony. B6.SJL-*Ptprc*<sup>a</sup> *Pepc*<sup>b</sup>/BoyJ and *R26-CreERT2* mice were originally from the Jackson Laboratory. C57BL/6J mice were purchased from The CLEA Japan. All mice were housed under SPF conditions. All animal experiments were done with the approval of the Animal Research Committee of Graduate School of Medicine, Kyoto University.

#### Cell culture and transfection

HEK293T cells were maintained in DMEM (nacalai tesque) supplemented with 10% fetal bovine serum (FBS) (Clontech). Tet-off HEK293 cells were cultured in  $\alpha$ -MEM (nacalai tesque) supplemented with 10% Tet-off system-approved FBS (Takara Bio) and 100 mg/ml G418 (nacalai tesque). Flp-In 293 T-Rex cells (Invitrogen) were grown in DMEM with 10% FBS and 2 mM L-glutamine. TSt-4 stroma cells were cultured in RPMI 1640 (nacalai tesque) supplemented with 10% FBS, 1 mM sodium pyruvate (Gibco), 0.1 mM non-essential amino acids solution (Gibco), 50 mM  $\beta$ -mercaptoethanol (nacalai tesque), 100 U/mL penicillin, and 100 mg/mL streptomycin (nacalai tesque). PEI MAX (Polysciences, Inc) was used for transfection following the manufacturer's protocol. For mRNA decay experiments with Tet-off system, Tet-off 293 cells were transfected with pTRE-tight vectors. Twenty-four hours post-transfection, doxycycline (2  $\mu$ g/ml) (Sigma) was added to the medium for the indicated time intervals before harvesting cells.

#### Flow Cytometry

Single cell suspensions were prepared from the BM and spleen and resuspended in FACS

buffer (5% BSA, 2mM EDTA in PBS). Single-cell suspensions were prepared and stained with fluorochrome-conjugated antibodies with the following specificities: CD3e (145-2C11), CD4 (GK1.5), CD8a (53-6.7), CD11b (M1/70), CD11c (N418), CD16/CD32 (2.4G2), CD19 (MB19-1), CD25 (PC61), CD34 (HM34), CD41 (MWReg30), CD61 (2C9.G2), CD45.1 (A20), CD45.2 (104), CD45R/B220 (RA3-6B2), CD48 (HM48-1), CD90.1 (HIS51), CD105 (MG7/18), c-Kit (2B8), IL-7Ra (A7R34), CD135 (A2F10), CD150 (TC15-12F12.2), CD201 (RCR-16), Sca-1 (D7), Ly-6D (49-H4), Ly-6G/Ly-6C (RB6-8C5), NK-1.1 (PK136), TCR b chain (H57-597), TER-119 (TER-119). For surface markers, staining was performed for 20 min at four degree. After washed twice, cells were stained with propidium iodide (PI) prior to FACS analysis. Except for staining with CD16/CD32 antibody, rat anti-mouse CD16/CD32 (Mouse BD Fc Block) was used to block FcRs. Stained cells were analyzed on an LSR Fortessa (BD Biosciences) and analyzed using FlowJo software (Tree Star).

For the identification of HSC and MPPs, BM cells were gated on lineage-negative (CD3, CD4, CD8, CD19, B220, CD11b, CD11c, Gr-1, Ter119, NK1.1), Sca1<sup>+</sup>, and Kit<sup>+</sup> (LSK). In FL transplantation experiments, LSK cells were further separated into Flt3<sup>-</sup>CD150<sup>+</sup> LSK and Flt3<sup>hi</sup>CD150<sup>-</sup> LMPP. In non-reconstitution mouse models, LSK were further separated into Flt3<sup>-</sup>CD150<sup>+</sup>CD48<sup>-</sup> LT-HSC, Flt3<sup>-</sup>CD150<sup>-</sup>CD48<sup>-</sup> ST-HSC, Flt3<sup>-</sup>CD150<sup>+</sup>CD48<sup>+</sup> MPP2, Flt3<sup>-</sup>CD150<sup>-</sup>CD48<sup>+</sup> MPP3, Flt3<sup>+</sup>CD150<sup>-</sup>CD48<sup>+</sup> MPP4 (Supplemental Figure 3C). CLP was identified as Flt3<sup>+</sup>IL-7R $\alpha$ <sup>+</sup>Lin<sup>-</sup>Sca1<sup>int-lo</sup>Kit<sup>int-lo</sup> population. Pre-GM, GMP, pre-Mk/E, and MkP progenitor populations were identified as Lin<sup>-</sup>Sca1<sup>-</sup>Kit<sup>+</sup> (LK). Pre-GMs were further gated as CD41<sup>-</sup>Fc $\gamma$ R<sup>-</sup>CD105<sup>-</sup>CD150<sup>-</sup>, GMP as CD41<sup>-</sup>Fc $\gamma$ R<sup>+</sup>CD150<sup>-</sup>, pre-Mk/E as CD41<sup>-</sup>Fc $\gamma$ R<sup>-</sup>CD105<sup>-</sup>CD150<sup>+</sup>, MkP as CD41<sup>+</sup>. Mature cell populations were defined as following: pro-B cells (IgM<sup>-</sup>IgD<sup>-</sup>CD25<sup>-</sup>Kit<sup>+</sup>CD19<sup>+</sup>B220<sup>+</sup>), pre-B cells (IgM<sup>-</sup>IgD<sup>-</sup>CD25<sup>+</sup>Kit<sup>-</sup>CD19<sup>+</sup>B220<sup>+</sup>), Immature B cells (IgM<sup>+</sup>IgD<sup>-</sup>CD19<sup>+</sup>B220<sup>+</sup>), mature B cells (IgM<sup>+</sup>IgD<sup>+</sup>CD19<sup>+</sup>B220<sup>+</sup>), granulocytes (Gr-1<sup>hi</sup>CD11b<sup>+</sup>), and monocytes (Gr-1<sup>int-lo</sup>CD11b<sup>+</sup>).

### **BrdU Incorporation Assay and Annexin V Staining**

For cell proliferation analysis, the BrdU Flow Kit (BD Pharmingen) was used according to the manufacturer's instructions. Mice were intraperitoneally injected with 100  $\mu$ g of BrdU 1 hour before the analysis. PBS injection was used as a negative control. FACS-sorted populations were stained with anti-BrdU antibodies. For apoptosis analysis, cells were stained with Annexin V (Biolegend) in Annexin buffer (10 mM HEPES (pH7.4), 140 mM NaCl, 2.5 mM  $\text{CaCl}_2$ ) along with 7-AAD. Flow cytometric analysis of these cells were performed by using LSR Fortessa (BD Biosciences).

### **Reconstitution experiments**

For the generation of full chimeras, FL cells were purified from E15.5 embryos (CD45.2) with the indicated genotypes. Cells were injected intravenously into lethally irradiated (10 Gy) congenic B6.SJL-Ptprc<sup>a</sup> Pepc<sup>b</sup>/BoyJ (CD45.1) mice. BM cells were analyzed at 4-6 weeks after transplantation. For competitive transplantation, FL cells from CD45.1 WT together with those either from CD45.2 control or *DKO* fetuses were 1:1 mixed and transplanted into lethally irradiated CD45.1/CD45.2 mice. Mice were sacrificed at 4-6 weeks after transplantation. The reconstitution efficiency was more than 95%. Cells were prepared from BM, thymus, and peripheral blood, and used for further experiments. For HSC reconstitution assays, CD45.1/CD45.2 recipient mice were lethally irradiated prior to transplantation (4.5 Gy  $\times$  2). 250 Flt3<sup>-</sup>CD48<sup>-</sup>CD150<sup>+</sup> LSK (LSK-SLAM) cells were sorted from CD45.2 CreERT2<sup>+</sup>*RegI*<sup>fl/+</sup>*Reg3*<sup>+/-</sup> or CreERT2<sup>+</sup>*RegI*<sup>fl/fl</sup>*Reg3*<sup>-/-</sup> mice 14 days after tamoxifen treatment and then transplanted into the recipient mice together with  $5 \times 10^5$  supportive total BM cells. For secondary transplantations,  $1 \times 10^6$  total BM cells were isolated and transplanted into lethally irradiated secondary recipients (CD45.1) (4.5 Gy  $\times$  2). Contribution of CD45.2 donor cells was monitored in peripheral blood every 4 weeks post transplantation using LSR Fortessa (BD Biosciences). Peripheral blood collections for assessment of donor chimerism were performed at 4, 8, and 12 weeks after primary and secondary transplantations. Cells were stained with antibodies to CD45.1, CD45.2,

CD11b, Gr-1, B220, CD19, CD4, CD8, and TCR- $\beta$ . Recipients with lower than 1% total chimerism were considered failed transplantations and excluded from analysis.

### **BM Preparation and Lineage Depletion**

BM cells were purified from femurs, tibias, humeruses and ilia by crushing bones with mortar and pestle in sterile PBS (nacalai tesque) supplemented with 2% BSA and 1mM EDTA. Red blood cells were lysed in BM cells with ACK lysing buffer (Thermo Fisher Scientific). Lin<sup>-</sup> cells or Kit<sup>+</sup> cells were purified using Lineage Cell Depletion Kit or anti-PE MicroBeads (Miltenyi Biotec) on LS MACS columns (Miltenyi Biotec). Cells were then used for subsequent experiments or sorted on FACS Aria III cell sorter (BD Biosciences).

### **Establishment of MPP<sup>hId3-ERT2</sup> Cells**

Id3-ERT2-expressing multipotent progenitor (MPP<sup>hId3-ERT2</sup>) cells were established as described previously.<sup>5</sup> Briefly, LSK cells were purified from BM of WT or *RegI<sup>fl/fl</sup>Reg3<sup>-/-</sup>ROSA<sup>yfp/+</sup>* mice, then retrovirally transduced with the plasmid expressing hId3-ERT2-IRES-GFP by spin-infection. Cells were cultured on TSt-4 stromal cells in IMDM (Gibco) supplemented with 10 ng/mL mSCF, 10 ng/mL mFlt3L, and 20 ng/mL mIL-7 (R&D) and 40 nM 4-OHT (Sigma). For B cell differentiation, cells were cultured on TSt-4 cells in IMDM supplemented with 5 ng/mL mIL-7 in the absence of 4-OHT. For in-vitro doxycycline-inducible cre expression, MPP<sup>hId3-ERT2</sup> cells were lentivirally transduced with pInducer20-tagBFP containing cre sequence, and treated with 2  $\mu$ g/mL doxycycline. For RNA-immunoprecipitation (RIP)-RT-qPCR assay, these cells were transduced with pInducer20-mCherry containing either FLAG-tagged Reg1 or Reg3. For retroviral overexpression, MPP<sup>hId3-ERT2</sup> cells were transduced with MSCV-Thy1.1 by spin infection. The infected cells were washed twice and cultured on TSt-4 cells for 6 days under B cell-differentiating condition.

### **Ex vivo HSC culture**

*Ex-vivo* HSC serum-free culture was performed as described previously.<sup>6</sup> Soluplus®

(polyvinyl caprolactam-polyvinyl acetate-polyethylene glycol graft copolymer) was kindly provided by S. Yamazaki.<sup>7</sup> Briefly, Kit<sup>+</sup> cells were isolated from the bone marrow of C57BL/6 mice by using anti-PE MicroBeads (Miltenyi Biotec). Cells were cultured in serum-free F12 medium (Life Technologies), supplemented with SCF (10 ng/mL; PeproTech), TPO (100 ng/mL; PeproTech), Insulin-Transferrin-Selenium-Ethanolamine (ITSX; 1%; Life Technologies), HEPES (10 mM; Gibco), and with Soluplus (0.1%). Media changes were performed three times a week. HSC quality was monitored by flow cytometry based on the expression of CD150, CD48, and CD201 in LSK population. For HSC stimulation, IL-1 $\beta$  or TNF were added at 25 ng/mL or 1 mg/mL, respectively.

### **Measurement of Lymphoid Lineage Potential**

B lymphocyte potential of purified progenitors was evaluated following co-culture on TSt-4 stromal cells. Lin<sup>-</sup>Kit<sup>+</sup>IL-7R $\alpha$ <sup>+</sup> cells were purified from FL cells at E16.5. Cells were then seeded onto stroma monolayers in 24-well plates and cultured in RPMI supplemented with 10 ng/mL mSCF, 10 ng/ml mFlt3L, and 10 ng/ml mIL-7 (PeproTech). For induction of cre recombinase, 4-OHT was added at 40 nM. On day 6 or day 7, cells were subjected to flow cytometry to assess generation of CD19<sup>+</sup> B cells and CD11b<sup>+</sup> myeloid cells.

### **Luciferase assay**

HEK293 or HeLa cells were transfected with mock or pGL3 plasmids containing various 3'UTR (listed in Supplementary Table S6), together with mock or expression plasmids for Reg1 and Reg3. After 24 h of cultivation, luciferase activities in the lysates were determined using the Dual-luciferase reporter assay system (Promega), according to the manufacturer's protocol. The Renilla luciferase gene was simultaneously transfected as an internal control.

### **Immunoblot analysis**

Whole-cell lysates were prepared in lysis buffer (1% (vol/vol) Nonidet P-40, 0.1% (wt/vol) SDS, 1% (wt/vol) sodium deoxycholate, 150mM NaCl, 20mM Tris-HCl, pH7.5,

and 1mM EDTA), supplemented with Complete Mini Protease Inhibitor Cocktail without EDTA (Roche)). Lysates were separated by SDS-PAGE and transferred to nitrocellulose membranes (BIO RAD). The following antibodies were used for immunoblot analysis: antibody against I $\kappa$ B- $\zeta$  (14-6801-80; Thermo), FLAG-tag (F3165; Sigma) or antibody against  $\beta$ -actin (sc-1615; Santa Cruz) serving as a loading control. Polyclonal rabbit Regnase-1 and monoclonal rat anti-Regnase-3 (4D3) antibodies were previously described.<sup>8,9</sup> Luminescence was detected with a luminescent image analyzer (ImageQuant LAS 4000; GE Healthcare).

### **Quantitative RT-PCR Analysis**

Total RNA was isolated using TRIzol (Thermo Fisher Scientific) or Dynabeads MyOne Silane (Thermo Fisher Scientific). Reverse-transcription (RT) was carried out using ReverTra Ace® qPCR RT Master Mix with gDNA Remover (TOYOBO) or SuperScript IV VILO Master Mix (Thermo Fisher Scientific). Quantitative PCR (qPCR) was performed with SYBR® Select Master Mix (Applied Biosystems). Fluorescence was detected with a StepOne Real-Time PCR System (Applied Biosystems). qPCR primers used are listed in supplemental Table 5.

### **mRNA stability**

Actinomycin D (5  $\mu$ g/ml) was added directly to cell cultures following treatment with IL-1 $\beta$  or LPS for 2 hours. Cells were harvested at the indicated time after the addition of actinomycin D, followed by RT-qPCR analysis of mRNA as described above.

### **RNA-immunoprecipitation (RIP)-RT-PCR**

Cells were washed in PBS and lysed in 1mL RNA IP lysis buffer (50 mM Tris-HCl, [pH 7.5], 150 mM KCl, 2 mM EDTA [pH 8.0], 0.5% NP-40, 0.5 mM DTT, complete EDTA-free protease inhibitor cocktail (Roche) and 0.2 U/ml RNasin (Promega)). After incubation on ice for 10 min, followed by centrifugation, 5% of the total lysates were stored for input RNA and immunoblot analysis. FLAG-conjugated Protein G magnetic beads (Thermo Fisher Scientific) were incubated with the lysates for 3 hours at 4 °C.



Beads were washed three times in RNA IP lysis buffer (50 mM Tris-HCl, [pH 7.5], 150 mM KCl, 0.5%, NP-40, 0.5 mM DTT and complete EDTA-free protease inhibitor cocktail (Roche)). RNA was eluted by adding RLT buffer (QIAGEN) directly to the beads, then extracted following the instructions of the manufacturer. RIP transcript levels were normalized to input transcript levels and enrichments calculated relative to 18S or RPL18A.

### **ASO Delivery**

For delivery of antisense morpholino oligonucleotides, HeLa cells or BM-derived macrophages were seeded in 24 well plate prior to transfection. Morpholinos were added to the medium at a final concentration of 2  $\mu$ M, followed by addition of 6  $\mu$ M Endo-Porter (Gene Tools, LLC). For luciferase assay, HeLa cells were transfected with pGL3 plasmid simultaneously using Lipofectamine LTX (Thermo Fisher Scientific). For the delivery of morpholinos into cultured HSCs, electroporation was performed using P3 Primary Cell 4D-Nucleofector™ X Kit (protocol # EO-100, Lonza Bioscience).

### **HITS-CLIP**

Flp-In 293 T-REx cell lines stably expressing FLAG/HA-tagged Reg3 were generated as previously described.<sup>10</sup> Expression of epitope-tagged proteins was induced by addition of 1  $\mu$ g/mL doxycycline. The expression of FLAG/HA-tagged Reg3 protein was assessed by immunoblot analysis using mouse anti-HA antibody (Covance). HITS-CLIP was performed essentially as described.<sup>11</sup> Briefly, UV-irradiated cells were lysed in NP-40 lysis buffer (50 mM HEPES-KOH at pH 7.4, 150 mM KCl, 2 mM EDTA, 0.5% (v/v) NP-40, 0.5 mM DTT, complete EDTA-free protease inhibitor cocktail). After treatment with RNaseT1 (Thermo Fisher Scientific) at final concentration of 0.5 unit/ $\mu$ L, immunoprecipitation was carried out with FLAG magnetic beads (SIGMA) from HEK293 cell extracts for 1 h at 4°C. Following additional digestion by RNase T1 at final concentration of 0.5 unit/ $\mu$ L, beads were incubated with calf intestinal phosphatase (NEB) and RNA fragments were radioactively end-labeled using T4 polynucleotide

kinase (Thermo Fisher Scientific). The crosslinked protein-RNA complexes were resolved on a 4-12% NuPAGE gel (Invitrogen). The SDS-PAGE gel was transferred to a nitrocellulose membrane (Whatman) and the protein-RNA complex migrating at an expected molecular weight was excised. RNA was isolated by Proteinase K (Roche) treatment and phenol-chloroform extraction, ligated to 3' adapter and 5' adapter, reverse transcribed and PCR-amplified. The amplified cDNA was sequenced on a HighSeq2000 (Illumina) with a  $1 \times 51$  nt cycle.

### **Massively parallel single-cell RNA sequencing library preparation**

Single-cell libraries were prepared as previously described.<sup>12,13</sup> Briefly, mRNA from cells sorted into cell capture plates was barcoded, converted to cDNA and pooled with an automated pipeline. The pooled sample was then linearly amplified by T7 in vitro transcription, and the resulting RNA was fragmented and converted to a sequencing-ready library by tagging the samples with pool barcodes and Illumina sequences during ligation, reverse transcription and PCR. Each pool of cells was tested for library quality, and the concentration was assessed as described. All RNA-seq libraries (pooled at equimolar concentrations) were sequenced on the Illumina NextSeq 500 platform at a median sequencing depth of 27,994 reads per cell. Sequences were mapped to the mouse genome (mm10), demultiplexed and filtered as described,<sup>12</sup> extracting a set of unique molecular identifiers that defined distinct transcripts in single cells for further processing. We estimated the level of spurious UMIs in the data with statistics on empty MARS-seq wells and excluded all plates with estimated noise of >5%. Mapping of reads was done with HISAT (v0.1.6); reads with multiple mapping positions were excluded. Reads were associated with genes if they were mapped to an exon, using the UCSC Genome Browser for reference. Exons of different genes that shared a genomic position on the same strand were considered to represent a single gene with a concatenated gene symbol. Cells with fewer than 500 UMIs were discarded from the analysis.

### **Construction of reference model**

Construction of the hematopoietic core reference models was done by the MetaCell package as previously described and deposited in the GitHub (<https://github.com/MetaCell>).<sup>14,15</sup> The MetaCell pipeline was used to derive informative genes and compute cell-to-cell similarity, to compute k-nearest neighbor (k-nn) graph covers and derive distribution of RNA in cohesive groups of cells (or meta-cells), and to derive strongly separated clusters using bootstrap analysis and computation of graph covers on resampled data. The hematopoietic core dataset was extracted from cells sorted from four sorting strategies enriching for Kit, Sca-1 and CD150, and depleting different groups of lineage markers. Cells were filtered for high expression of gene sets of the following excluded lineages: ILC (*Ccl5*), megakaryocytes (*Pf4*), erythrocytes (*Car1* and *Hba-a2*), basophils (*Prss34*) and eosinophils (*Prg2*), B cells (*Vpreb1* and *Fcrla*), neutrophils (*Ltf* and *Fcnb*), macrophages (*C1qb*), and DC (*Cd74* and *Siglech*). This resulted in filtering 7,075 cells and retaining 9,348 cells for further analysis. Clustering was performed using MetaCell analysis (but excluding specifically the strong neutrophil differentiation module, including *Camp*, *Ltf*, *S100a8*, *S100a9*, and the hemoglobin genes *Hba-a2*, *Hbb-b1* and *Beta-s*), using bootstrap to derive robust clustering (resampling 70% of the cells in each iteration, and clustering the co-cluster matrix with minimal cluster size set to 20, and number of bootstrap clusters set to 50).

### **Projection of sorted cells**

LSK cells from WT and *DKO* mice were projected onto the hematopoietic core reference model as described below. Projected cells were filtered for high expression of gene sets of the following excluded lineages: ILC (*Ccl5*), megakaryocytes (*Pf4*), erythrocytes (*Car1* and *Hba-a2*), basophils (*Prss34*) and eosinophils (*Prg2*), B cells (*Vpreb1* and *Fcrla*), neutrophils (*Ltf* and *Fcnb*), macrophages (*C1qb*), and DC (*Cd74* and *Siglech*), retaining 2241 WT and 2242 *DKO* cells. We extracted for each projected cell the 10 reference cells with top Pearson's correlation over the normalized gene features defined for the reference model. The distribution of cluster memberships over these k-neighbors

was used to associate the new cell with a reference meta-cell (by majority voting) and to project the cell in two dimensions by weighted average of the linked reference clusters' mapped x and y coordinates. To exclude the possibility of variations that might have occurred between the sorting plates of WT and *DKO*, no significant difference in the distribution of meta-cells between the sorting plates was confirmed (supplemental Figure 5A).

### **scATAC-seq**

Flt3<sup>-</sup>CD48<sup>-</sup> LSK cells were sorted as described above. Nuclei isolation for scATAC-seq was performed according to the "Nuclei Isolation for Single Cell ATAC Sequencing Demonstrated Protocol" (10x Genomics). After nuclei isolation, nuclei pellet was suspended in 1× Nuclei Buffer (10x Genomics) and used according to the Chromium Single Cell ATAC Reagent Kits User Guide (10x Genomics). Briefly, nuclei suspensions were incubated in the tagmentation mix for 1 hour at 37 °C. After mixing with a barcoding mix, the nuclei were loaded into a 10x chip H together with barcoded beads and partitioning oil (Chromium Next GEM Chip H Single Cell Kit v1.1, Chromium Next GEM Single Cell ATAC Library & Gel Bead Kit v1.1, 10x Genomics) and encapsulated using the Chromium controller (10x Genomics). The Gel Bead-In Emulsions (GEMs) was transferred into a PCR tube and amplified for 12 cycles in a thermocycler. The barcoded DNA was purified and subjected to an index PCR for 9 cycles. The library amplification was assessed using High Sensitivity DNA chip (Agilent) and sequenced on an Illumina NovaSeq 6000 system using S1 Reagent Kit v1.5 (100cycles) in PE mode (50 × 8 × 16 × 50 read lengths).

### **Analysis of scATAC-seq data**

scATAC-seq base call files (BCLs) for each sample were processed into FASTQ files and count data using cellranger-atac mkfastq and cellranger-atac count, as provided by 10x Genomics (version 2.0.0). Data for the four samples were merged using cellranger-atac aggr. Mouse reference data was obtained from the 10x Genomics website (version mm10-

2020-A-2.0.0). The thus obtained feature-to-barcode count matrix and fragment data was further analyzed using the R packages, Seurat (version 4.1.0),<sup>16</sup> Signac (version 1.5.0),<sup>17</sup> EnsDb.Mmusculus.v75 (version 2.99.0)<sup>18</sup>. Peaks present in fewer than ten cells, and cells with fewer than 200 peaks were removed, resulting in a dataset of 195,171 peak loci and 41,606 cells. Additional filtering was performed as follows: we filtered out cells with < 3,000 or > 20,000 fragments inside peak regions, cells with < 30% of fragments inside peak regions, cells with a nucleosome signal > 4 (function NucleosomeSignal), and cells with a TSS enrichment score < 2 (function TSSEnrichment). This resulted in a dataset of 35,160 remaining cells. Normalization was performed using term frequency-inverse document frequency normalization (function RunTFIDF). Linear dimensionality reduction was performed by using singular value decomposition (function RunSVD) on all peak regions, followed by non-linear dimensionality reduction using uniform manifold approximation and projection (UMAP, function RunUMAP) based on the 2<sup>nd</sup> to 30<sup>th</sup> latent semantic indexing (LSI) components. The first LSI component was omitted because it was strongly anticorrelated with sequencing depth (function DepthCor). Clustering of cells was performed using the functions FindNeighbors (using the 2<sup>nd</sup> to 30<sup>th</sup> LSI) and FindClusters using the smart local moving (SLM) algorithm.

The chromatin accessibility of genes was estimated using the GeneActivity function, which sums the fragments inside the gene body and promoter region (upstream 2kb) of every gene, followed by normalization of this data (function NormalizeData using the total fragment count in each cell as a scale factor, and otherwise default parameters). Accessibility in genomic regions were visualized using function CoveragePlot. Differentially accessible regions (DARs) between clusters were predicted using the FindMarkers function (parameter test.use set to 'LR' and otherwise default parameters). For the prediction between C7 and C8 additional parameters min.pct and logfc.threshold were set to 0.05 and 0.1 respectively.

Enrichment of transcription factor binding site (TFBS) motifs in sets of DARs

was analyzed using R packages JASPAR2020 (version 0.99.10)<sup>19</sup>, TFBSTools (version 1.32.0)<sup>20</sup>, and BSgenome.Mmusculus.UCSC.mm10 (version 1.4.3)<sup>21</sup>. TFBS motif data was added to the Seurat object using the functions getMatrixSet and Addmotifs, and enriched motifs were predicted using the FindMotifs function. To avoid biases caused by differences in GC content, we used function AccessiblePeaks and MatchRegionStats to define a set of peak regions for generating reference sets with matched GC content, which was given as input to the FindMotifs function.

Gene Ontology (GO) term enrichment analysis was performed as follows. Genes located closest to DARs (with avg\_log2FC > 0.2) were picked up using function ClosestFeature, and given as input to the R package GStats (version 2.60.0)<sup>22</sup>. As gene universe we used all genes in the Seurat object. Genes were converted to Entrez ids using annotation data in R package org.Mm.eg.db (version 3.14.0)<sup>23</sup>, and enriched GO terms were predicted using the function hyperGTest. The codes used for the analysis of scATAC-seq data were deposited in the GitHub ([https://github.com/alexisvdb/Uehata\\_scATAC](https://github.com/alexisvdb/Uehata_scATAC)).

### **Statistical Analysis**

The variations of data were presented as the means with standard deviations (SDs) or standard errors of the mean (SEMs). A *p* value of < 0.05 was considered significant. For comparison of two groups, a two-tailed unpaired Student's *t*-test for parametric variables was used. For comparisons of multiple groups, one-way ANOVA followed by the Holm-Sidak-corrected two-tailed *t*-tests was used. The statistical analysis indicated in the figure legends were performed with GraphPad Prism Software (GraphPad Inc., La Jolla, CA). Additional information about experimental procedures is presented in the Supplemental information.

### **References**

1. Okuma A, Hoshino K, Ohba T, et al. Enhanced apoptosis by disruption of the STAT3-IkappaB-zeta signaling pathway in epithelial cells induces Sjogren's syndrome-like autoimmune disease. *Immunity*. 2013;38(3):450-460.



2. Schlenner SM, Madan V, Busch K, et al. Fate mapping reveals separate origins of T cells and myeloid lineages in the thymus. *Immunity*. 2010;32(3):426-436.
3. Matsushita K, Takeuchi O, Standley DM, et al. Zc3h12a is an RNase essential for controlling immune responses by regulating mRNA decay. *Nature*. 2009;458(7242):1185-1190.
4. Uehata T, Iwasaki H, Vandenbon A, et al. Malt1-induced cleavage of regnase-1 in CD4(+) helper T cells regulates immune activation. *Cell*. 2013;153(5):1036-1049.
5. Ikawa T, Masuda K, Huijskens M, et al. Induced Developmental Arrest of Early Hematopoietic Progenitors Leads to the Generation of Leukocyte Stem Cells. *Stem Cell Reports*. 2015;5(5):716-727.
6. Wilkinson AC, Ishida R, Kikuchi M, et al. Long-term ex vivo haematopoietic-stem-cell expansion allows nonconditioned transplantation. *Nature*. 2019;571(7763):117-121.
7. Becker HJ, Ishida R, Wilkinson AC, et al. A Single Cell Cloning Platform for Gene Edited Functional Murine Hematopoietic Stem Cells. *bioRxiv*. 2022:2022.2003.2023.485423.
8. Iwasaki H, Takeuchi O, Teraguchi S, et al. The IkappaB kinase complex regulates the stability of cytokine-encoding mRNA induced by TLR-IL-1R by controlling degradation of regnase-1. *Nat Immunol*. 2011;12(12):1167-1175.
9. von Gamm M, Schaub A, Jones AN, et al. Immune homeostasis and regulation of the interferon pathway require myeloid-derived Regnase-3. *J Exp Med*. 2019;216(7):1700-1723.
10. Mino T, Murakawa Y, Fukao A, et al. Regnase-1 and Roquin Regulate a Common Element in Inflammatory mRNAs by Spatiotemporally Distinct Mechanisms. *Cell*. 2015;161(5):1058-1073.
11. Hafner M, Landthaler M, Burger L, et al. Transcriptome-wide identification of RNA-binding protein and microRNA target sites by PAR-CLIP. *Cell*. 2010;141(1):129-141.
12. Jaitin DA, Kenigsberg E, Keren-Shaul H, et al. Massively parallel single-cell RNA-seq for marker-free decomposition of tissues into cell types. *Science*. 2014;343(6172):776-779.
13. Keren-Shaul H, Kenigsberg E, Jaitin DA, et al. MARS-seq2.0: an experimental and analytical pipeline for indexed sorting combined with single-cell RNA sequencing. *Nat Protoc*. 2019;14(6):1841-1862.
14. Giladi A, Paul F, Herzog Y, et al. Single-cell characterization of haematopoietic progenitors and their trajectories in homeostasis and perturbed haematopoiesis. *Nat Cell Biol*. 2018;20(7):836-846.
15. Baran Y, Bercovich A, Sebe-Pedros A, et al. MetaCell: analysis of single-cell RNA-seq data using K-nn graph partitions. *Genome Biol*. 2019;20(1):206.
16. Hao Y, Hao S, Andersen-Nissen E, et al. Integrated analysis of multimodal single-cell data. *Cell*. 2021;184(13):3573-3587 e3529.
17. Stuart T, Srivastava A, Madad S, Lareau CA, Satija R. Single-cell chromatin state analysis

with Signac. *Nat Methods*. 2021;18(11):1333-1341.

18. Rainer J (2017). *EnsDb.Mmusculus.v75: Ensembl based annotation package*. R package version 2.99.0.

19. Fornes O, Castro-Mondragon JA, Khan A, et al. (2019). JASPAR 2020: update of the open-access database of transcription factor binding profiles. *Nucleic Acids Res.* 48, D87-D92.

20. Tan G, Lenhard B (2016). “TFBSTools: an R/Bioconductor package for transcription factor binding site analysis.” *Bioinformatics*, **32**, 1555-1556.

21. Team TBD (2021). *BSgenome.Mmusculus.UCSC.mm10: Full genome sequences for Mus musculus (UCSC version mm10, based on GRCm38.p6)*. R package version 1.4.3.

22. Falcon S, Gentleman R (2007). “Using GOstats to test gene lists for GO term association.” *Bioinformatics*, **23**(2), 257-8.

23. Carlson M (2019). *org.Mm.eg.db: Genome wide annotation for Mouse*. R package version 3.8.2.

Supplemental Table 4. Significant overlap between Reg1 and Reg3 HITS-CLIP peaks

RBP1		RBP2		Number 3'UTR	Number of peaks RBP1	Number of peaks RBP2	Observed Overlap	Expected Overlap	P- value	Z- score	Fold Enrichment
Reg1	replicate1	Reg3	replicate1	5894	683	8605	106	9.94	1E-212	31.1	10.7
Reg1	replicate1	Reg3	replicate2	3680	683	4750	47	7.71	1E-45	14.2	6.10
Reg1	replicate2	Reg3	replicate1	6670	3157	8605	435	44.243	1E-767	59.4	9.83
Reg1	replicate2	Reg3	replicate2	4901	3157	4750	193	29.744	1E-210	31.0	6.49